The comparative characterization of structural heterogeneity of mesoporous activated carbon fibers (ACFs)

Piotr Kowalczyk[a], Vladimir M. Gun'ko[b], Artur P. Terzyk[c,*], Piotr A. Gauden[c], Haiqin Rong[d], Zhenyu Ryu[d], Duong D. Do[e]

[a]*Department of Respiratory Protection, Military Institute of Chemistry and Radiometry, gen. Chruściel Avenue 105, Warsaw 00-910, Poland*
[b]*Institute of Surface Chemistry, 17 General Naumov Street, Kiev 03164, Ukraine*
[c]*Department of Chemistry, Physicochemistry of Carbon Materials Research Group, N. Copernicus University, Gagarin Street 7, Toruń 87-100, Poland*
[d]*Institute of Coal Chemistry, Chinese Academy of Sciences, PO Box 165, Taiyuan 030001, PR China*
[e]*Department of Chemical Engineering, The University of Queensland, St. Lucia, Qld 4072, Australia*

Abstract

The comparative analysis of the most widely used methods of mesoporosity characterization of two activated carbon fibers is presented. Not only the older methods are used, i.e. Barrett, Joyner and Halenda (*BJH*), Dubinin (the so-called first variant—D_{1ST} and the so-called second variant—D_{2ND}), Dollimore and Heal (*DH*), and Pierce (*P*) but the recently developed ones, i.e. the method of Nguyen and Do (*ND*) and that developed by Do (*Do*) are also applied. Additionally, the method of the characterization of fractality is put to use (fractal analog of FHH isotherm). The results are compared and discussed.
© 2002 Elsevier Science B.V. All rights reserved.

Keywords: Carbon fibers; Mesoporosity characterization; Pore size distribution; Fractal dimension

1. Introduction

Porous materials are usually heterogeneous both structurally and energetically. Among porous solids used in industry, activated carbons are the most complex ones. On the other hand, they are the most versatile due to their extremely high surface area and micropore volume. Activated carbon fibers (ACFs) are relatively novel fibrous adsorbents produced for example from pitch, cellulose, phenol resin and polyacrylonitryle [1–5]. Such a new generation of carbon materials can be utilized in different branches of chemistry, technology and industry. The adsorption/desorption characteristics of ACFs exhibit different behaviour according to the type of precursor used. The main advantage of these materials is a small fiber diameter, which minimizes diffusion limitations and allows rapid adsorption/desorption [6]. Typically, ACFs are characterized by a relatively narrow pore size distribution, very good mechanical properties (i.e. resistance to

* Corresponding author. Tel.: +48-056-660-74-12; fax: +48-056-654-2477.
E-mail address: aterzyk@chem.uni.torun.pl (A.P. Terzyk).

abrasion, ability to form different shapes) and excellent adsorption capacity at low concentration comparing to commercial activated granular/powder carbons [7]. ACFs appear to be very promising materials for adsorption from solutions. As reported by Tamai et al., ACFs obtained from organometallics/pitch composites have excellent adsorption properties for larger molecules in the liquid phase [8].

The pore size distribution (PSD) of ACFs, together with the chemical composition of the surface layer, are perhaps the most important characteristics, that affect the transport and adsorption equilibrium. Other structural characteristics of the mentioned materials (for example, a specific surface area, a micropore/mesopore volume, mean micropore/mesopore radius and others) can be obtained from the PSD curve.

In the present study, some conventional and new (developed recently) methods of estimating PSD from a singe nitrogen adsorption isotherm were adopted for characterizing ACFs. Not only the most popular older methods but also the newest ones are applied and the results are compared. What is also important is that the new numerical algorithm (called adsorption stochastic algorithm, ASA) for the calculation of the results from Nguyen and Do method is presented. Additionally, fractal analysis is used to study the surface roughness. The results are compared with those calculated using one of the newest method of porosity characterization, namely DFT theory. The main attention of the authors is paid to the comparative analysis of the methods of mesoporosity characterization.

2. Experimental

2.1. Adsorbents

Both activated carbon fibers were prepared following the method described in details previously [4,5].

2.2. Nitrogen adsorption measurements

A Micromeritics ASAP 2000 (Micrometics Ins. Corp.) was used to measure nitrogen adsorption isotherms at 77.5 K. High purity nitrogen (99.99%) was used and before each measurement the samples were desorbed at 573.15 K for 2 h [4,5].

3. The methods of calculation

To compute the mesopore size distribution curves (MPSDs), a few iterative methods based on Cohan's capillary condensation model (i.e. Barrett, Joyner and Halenda (*BJH*) [9], Dubinin (the so-called first variant–D_{IST} [10] and the so-called second variant—D_{2ND} [11]), Dollimore and Heal (*DH*) [12], and Pierce (*P*) [13]) were used in the present study. All above mentioned methods are characterized with the computational algorithm described in details by Jagiełło and Klinik [14]. If we denote for the *n*-th stage of desorption ΔV_n (cm^3/g) as a change in the adsorption value (of liquid adsorbate); $\bar{r}_n$ (cm) as the average pore diameter; $\bar{r}_{kn}$ (cm) as the average Kelvin's radius of the space between adsorbed layers; $\bar{t}_n$ (cm) as the average thickness of the adsorbed layer; Δt_n (cm) as the change in the thickness of the layer adsorbed on the pore walls for the considered stage of desorption; the change in the volume of empty pores for *n*-th stage of desorption ΔV_p (cm^3/g) is given by the following equations.

(I) For the method of Barrett, Joyner and Halenda (*BJH*) [9]:

$$\Delta V_p = \Delta V_n R_n - C \Delta t_n R_n \sum_{i=1}^{n-1} \frac{2\Delta V_{pi}}{\bar{r}_i} \qquad (1a)$$

where

$$R_n = \left(\frac{\bar{r}_n}{\bar{r}_{kn} + \Delta t_n}\right)^2 \qquad (1b)$$

$$C = \frac{\bar{r}_n - t}{\bar{r}_n} \qquad (1c)$$

(II) For the first variant of Dubinin's method (D_{IST}) [10]:

$$\Delta V_p = \Delta V_n + \bar{t}_n \frac{2\Delta V_n}{\bar{r}_{kn}} - \Delta t_n \sum_{i=1}^{n-1} \frac{2\Delta V_i}{\bar{r}_{ki}} \qquad (2)$$

(III) For the second variant of Dubinin's method (D_{2ND}) [11]:

$$\Delta V_p = \left(\Delta V_n - \Delta t_n \sum_{i=1}^{n-1} \frac{2\Delta V_i}{r_{ki}}\right)\left(\frac{\bar{r}_n}{\bar{r}_{kn}}\right)^2 \qquad (3)$$

(IV) For the method of Dollimore and Heal (*DH*) [12]:

$$\Delta V_p = \left(\Delta V_n - \Delta t_n \sum_{i=1}^{n-1} \frac{2\Delta V_{pi}}{\bar{r}_i} + \Delta t_n \bar{t}_n \sum_{i=1}^{n-1} \frac{2\Delta V_{pi}}{\bar{r}_i^2} \right)$$
$$\times \left(\frac{\bar{r}_n}{\bar{r}_{kn} + \Delta t_n} \right)^2 \qquad (4)$$

(V) For Pierce's method (*P*) [13]:

$$\Delta V_p = \left(\Delta V_n - \Delta t_n \sum_{i=1}^{n-1} \frac{2\Delta V_{pi}}{\bar{r}_i} \right) \left(\frac{r_n}{r_{kn}} \right)^2 \qquad (5)$$

Calculation of ΔV_p at each step of desorption makes it possible to calculate the differential pore volume $\Delta V_p/\Delta r$ and to draw the differential pore distribution curve for an adsorbent [15]:

$$\frac{\Delta V_p}{\Delta r} = f(\bar{r}) \qquad (6)$$

where $f(\bar{r})$ is a distribution function.

Additionally, the volume of mesopores can be calculated:

$$V_{mes} = \sum_{i=1}^{n} \Delta V_{pi} \qquad (7)$$

and the surface of mesopores:

$$S_{mes} = \sum_{i=1}^{n} \frac{2\Delta V_{pi}}{\bar{r}_i} \qquad (8)$$

In the current study, we also applied the method of Derjaguin–Broekhoff and de Boer, modified by Dubinin and Ulin. This method originates from the pioneering paper of Derjaguin [16] and, actually, is the modification of the Broekhoff and deBoer's method [17–23]. In this modification Dubinin and co-workers assumed that the surface tension of an adsorbate is the function of the radius of the curvature of meniscus of adsorbed nitrogen. They obtained the following equations [24]:

$$\log\left(\frac{p_s}{p}\right) - \left(\frac{16.11}{t_e^2}\right) + 0.1682 \exp(-0.1137 t_e)$$
$$= \frac{2.025}{r - t_e - 3.31} \qquad (9)$$

and

$$r - t_e = \frac{4.05(r - t_e)}{(r - t_e - 6.62)\log(p_s/p)} + \frac{1}{(r - t_e)\log(p_s/p)}$$
$$\times \left\{ 32.22 \left[\frac{r}{t_e} - 1 - \log\left(\frac{r}{t_e}\right) \right] \right.$$
$$- 2.964(r - t_e - 8.795)\exp(-0.1137 t_e)$$
$$\left. - 26.06 \exp(-0.1137 r) \right\} \qquad (10)$$

where p and p_s denote the equilibrium pressure and the saturation vapor pressure, respectively, t_e is the average thickness of the adsorbed layer and r the mesopore radius.

Thus, the pore size distributions in this case can be calculated taking into account in Eq. (3) the relationships (9) and (10), and this method is denoted as Derjaguin–Broekhoff–deBoer–Dollimore–Dubinin–Ulin (*DBdBDDU*).

Another method considered in this study was proposed by Nguyen and Do (*ND*) [25–28] and recently developed by Do [29–31]. They developed a new promising procedure for the evaluation of pore size distribution from adsorption data. Such a procedure is based on the combination of the Kelvin equation and the statistical adsorbed film thickness. The most important feature of this method is the possibility of analysis of the structural heterogeneity of porous solids without the need to distinguish the micropore range and the mesopore range. Additionally, it provides almost the same results as those obtained using the most sophisticated method of porosity characterization, namely the DFT method [25–32].

Following Nguyen and Do, the overall adsorption isotherm equation possesses the form as follows:

$$a = \int_{r_{min}}^{r_k(p)} f(R_p)\, dR_p$$
$$+ \int_{r_k(p)}^{r_{max}} \frac{w}{(R_p - \sigma_s)/2} t(p, R_p) f(R_p)\, dR_p \qquad (11)$$

where r_{min} and r_{max} are the minimal and maximal half widths (or pore radii), respectively; $w_{NG} = 1$ for slit like pores and 2 for cylindrical pores; $r_k(p)$ is determined with the Kelvin equation (γ is the liquid surface tension; v_m the liquid molar volume; θ the liquid–solid

contact angle; R the universal gas constant; T the temperature)

$$r_{k}(p) = \frac{\sigma_{s}}{2} + t(p, R_{p}) + \frac{w_{NG}\gamma v_{m}\cos\theta}{RT\log(p_{s}/p)} \tag{12}$$

where the statistical adsorbed film thickness is equal

$$t(p, R_{p}) = t_{m}\frac{c_{B}z_{B}}{1 - z_{B}}\left[\frac{1 + (n_{B}b/2) - (n_{B}/2)z_{B}^{n-1} - (n_{B}b + 1)z_{B}^{n} + (n_{B}/2) + (n_{B}/2)z_{B}^{n+1}}{1 + (c_{B} - 1)z_{B} + (c_{B}b/2 - b/2)z_{B}^{n} - (c_{B}b/2 + b/2)z_{B}^{n+1}}\right] \tag{13}$$

to $t_{m} = a_{m}/S_{BET}$ (thickness of a single layer of the adsorbate); a_{m} is the BET monolayer capacity; S_{BET} the BET specific surface area; $b = \exp(\Delta\varepsilon/RT)$; $\Delta\varepsilon$ the excess of the evaporation heat due to the interference of the layering on the opposite wall of pores ($\Delta\varepsilon \approx 2.2$ kJ mol^{-1}); $c_{B} = c_{s,B}\exp[(Q_{p} - Q_{s})/RT]$; $c_{s,B}$ is the BET coefficient for adsorption on a "flat" surface; Q_{s} and Q_{p} are the adsorption heats on a flat surface and in pores, respectively; $z_{B} = p/p_{s}$; n_{B} is the number (non-integer) of statistical monolayers of adsorbate molecules and its maximal value for the given R_{p} (or pore half width x) is equal to $(R_{p} - \sigma_{s}/2)/t_{m}$; and σ_{s} the collision diameter of surface atoms ($\sigma_{s} = 0.34$ nm for C atoms on carbon surfaces).

The fractional filling of pore (i.e. local adsorption isotherm) having half width R_{p} is defined as the ratio of the thickness $t(p, R_{p})$ to the maximum allowable physical half width $(R_{p} - \sigma_{s}/2)$, which is:

$$\theta(p, R_{p}) = \begin{cases} \dfrac{t(p, R_{p})}{R_{p} - \sigma_{s}/2}, & \text{for } p < p^{*} \\ 1, & \text{for } p \geq p^{*} \end{cases} \tag{14}$$

where p^{*} is the critical pressure at which the pore filling occurs and it is obtained from the solution of modified Kelvin equation. Thus, the problem of the solution of unstable linear Fredholm integral equation of the first kind may be replaced by a classical optimization problem with constraints.

Since in the present paper the new algorithm is applied to solve this problem we describe it in details below. In general case, we can define an expression describing a global adsorption isotherm as follows [26,33]:

$$\Psi_{t}(p_{j}) = \int_{x_{min}}^{x_{max}} g_{theor}(x_{i}, p_{j})f(x) \cong \sum_{i=1}^{N} w_{i}g_{theor}(x_{i}, p_{j}) \tag{15}$$

where $i = 1, 2, \ldots N$; $j = 1, 2, \ldots M$; x describes the structural heterogeneity of an adsorbent; $f(x)$ is the distribution function of a parameter x; $g_{theor}(x_{i}, p_{j})$ the discrete form of a local adsorption isotherm (i.e. kernel) that describes the adsorption process in homogenous pores; x_{min} is the smallest and x_{max} is the largest value of a structural parameter (i.e. pore with, radius, half width). Based on both the theory of nonlinear minimization and static penalty function our task is to find $\bar{w}$ so as to minimize functional $\Omega(\bar{w})$. Mathematically:

$$\text{mimise } \Omega(\bar{w}) = \begin{cases} \displaystyle\sum_{j=1}^{M}\left(\Psi_{t}(p_{j}) - \sum_{i=1}^{N} w_{i}g_{theor}(x_{i}, p_{j})\right)^{2}, & \text{if } \bar{w} \in \Xi \cap S \\ \displaystyle\sum_{j=1}^{M}\left(\Psi_{t}(p_{j}) - \sum_{i=1}^{N} w_{i}g_{theor}(x_{i}, p_{j})\right)^{2} + \sum_{i=1}^{H} C_{i}\delta_{i}, & \text{otherwise} \end{cases} \tag{16}$$

with respect to $\bar{w} = (w_{1}, w_{2}, \ldots, w_{N}) \in R^{N}$ where

$$\begin{cases} \delta_{i} = 1, & \text{if constraint ``}i\text{'' is violated} \\ \delta_{i} = 0, & \text{if constraint ``}i\text{'' is satisfied} \end{cases} \tag{17}$$

where H is the number of constraints, $\bar{w} \in \Xi \cap S$. The set $S \subseteq R^{N}$ defines the search space and the set $\Xi \subseteq R^{N}$ defines a feasible search space. The search

space S is defined as a N-dimensional rectangle in R^N (domains of variables defined by their lower and upper bounds)

$$l(i) \leq w_i \leq u(i), \quad 1 \leq i \leq N \tag{18}$$

The feasible search space Ξ was assumed outside the defined N-dimensional rectangle. It is noted that $\Omega(\bar{w})$ is the penalized objective function and C_i is a constant imposed for the violation of the constraint i. It is worthwhile to point out that such defining of a minimization problem always gives rise to physical solutions (i.e. negative value of distribution function $f(x)$, unphysical oscillations of distribution function $f(x)$, are avoided). We have defined a minimization problem of functional $\Omega(\bar{w})$, and we now turn to developing a minimization procedure. Obviously, for extracting $f(x)$ from measured global adsorption isotherm we can use genetic algorithms, evolutionary algorithms, simulated annealing, taboo search, deterministic algorithms (i.e. simplex strategy of Nelder and Mead, strategy of Hook and Jeeves, and so on), gradient methods (i.e. simple gradient method and so on), and hybrid methods [34]. All the above mentioned techniques determine all the unknown variables simultaneously. Developed by us and analyzed in this study are the new adsorption stochastic algorithm [35], the well-known relaxation (successive variation of the variables, parallel axis search, Gauss–Seidel strategy, alternating variable search, sectioning method [36]). The main idea of such minimization procedure is the sequential minimization problem of one dimension (i.e. minimize only one element from $\bar{w}$ vector). So the optimization is first carried out by only optimizing the first element of the $\bar{w}$ vector. Once w_1 is optimized, w_2 is then optimized next until w_k has been optimized. Once this is completed, the process is then repeated until no further change in the functional is observed. In the developing ASA program the well-known Rechenberg–Schwefel, Fibonacci division, and golden section procedures [37] were used for searching a local minimum in one dimension. All the procedures give very similar results.

Additionally, in the present study, the mesopore size distribution was calculated using the new method described in details by Do (Do) [38]. For the evaluation of the pore volume distribution of investigated ACFs, a bi-modal model of mesoporous structure was assumed. Following Do, the mesopore volume distribution was approximated by the combination of two gamma-type distributions:

$$f(r) = V_{S,1} \frac{\alpha_1^{p_1+1}}{\Gamma(p_1+1)} r^{p_1} \exp(-\alpha_1 r)$$
$$+ V_{S,2} \frac{\alpha_2^{p_2+1}}{\Gamma(p_2+1)} r^{p_2} \exp(-\alpha_2 r) \tag{19}$$
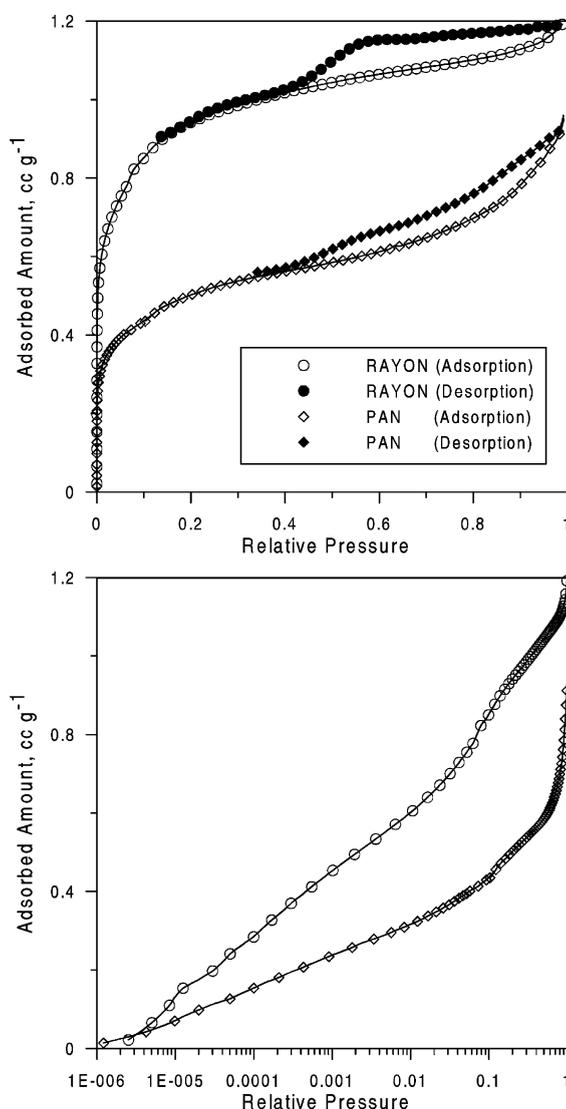

Fig. 1. Experimental adsorption–desorption isotherms of nitrogen at 77.5 K on the Rayon and PAN activated carbon fibers.

Therefore, the amount adsorbed in mesopores is equal to:

$$V(p) = V_{S,1} \frac{\Gamma(p_1 + 1, \alpha_1 r)}{\Gamma(p_1 + 1)} + V_{S,2} \frac{\Gamma(p_2 + 1, \alpha_2 r)}{\Gamma(p_2 + 1)}$$
$$+ 2V_{S,1}(\alpha_1 t) \left[\frac{\Gamma(p_1, \alpha_1 r_{\max})}{\Gamma(p_1 + 1)} - \frac{\Gamma(p_1, \alpha_1 r)}{\Gamma(p_1 + 1)} \right]$$
$$+ 2V_{S,2}(\alpha_2 t) \left[\frac{\Gamma(p_2, \alpha_2 r_{\max})}{\Gamma(p_2 + 1)} - \frac{\Gamma(p_2, \alpha_2 r)}{\Gamma(p_2 + 1)} \right] \tag{20}$$

where Γ denotes gamma function, $V_{S,j}$ is the j-th total pore volume, p_j and α_j are the j-th pore structural parameters, t is generally used as an estimate for the statistical adsorbed film thickness as a function of pressure for nitrogen adsorption at 77.5 K:

$$t = 0.354 \left[\frac{5}{\ln(p_s/p)} \right]^{1/3} \tag{21}$$

where 0.354 nm is the thickness of one nitrogen molecule. The threshold radius corresponding to a gas phase of pressure p is equal to:

$$r(p) = \begin{cases} t + \dfrac{2v_m \gamma \cos\theta}{RT \ln(p_s/p)}, & \text{for desorption} \\[2mm] t + \dfrac{v_m \gamma}{RT \ln(p_s/p)}, & \text{for adsorption} \end{cases} \tag{22}$$

Table 1
Main characteristics of the activated carbon fibers used in this study

| Theoretical model	Parameter	Rayon	PAN
n-BET (0.05 $< p/p_0 < 0.25$)	a_m (cc g^{-1})	0.88	0.50
	C	87.77	40.17
	n	1.59	1.53
	SSD	7.9E−5	2.6E−5
FHH (0.54 $< p/p_0 < 0.98$)	κ	1.1868	1.1254
	D	2.97	2.86
	SSD	5.1E−4	3.5E−3
Barrett, Joyner and Halenda (desorption branch)	V_{mes} (cc g^{-1})	0.66	0.48
	S_{mes} (m^2 g^{-1})	880	307
Dubinin (first variant) (desorption branch)	V_{mes} (cc g^{-1})	0.58	0.52
	S_{mes} (m^2 g^{-1})	722	305
Dubinin (second variant) (desorption branch)	V_{mes} (cc g^{-1})	0.55	0.49
	S_{mes} (m^2 g^{-1})	688	286
Dollimore and Heal (desorption branch)	V_{mes} (cc g^{-1})	0.58	0.51
	S_{mes} (m^2 g^{-1})	733	298
Pierce (desorption branch)	V_{mes} (cc g^{-1})	0.52	0.48
	S_{mes} (m^2 g^{-1})	638	278
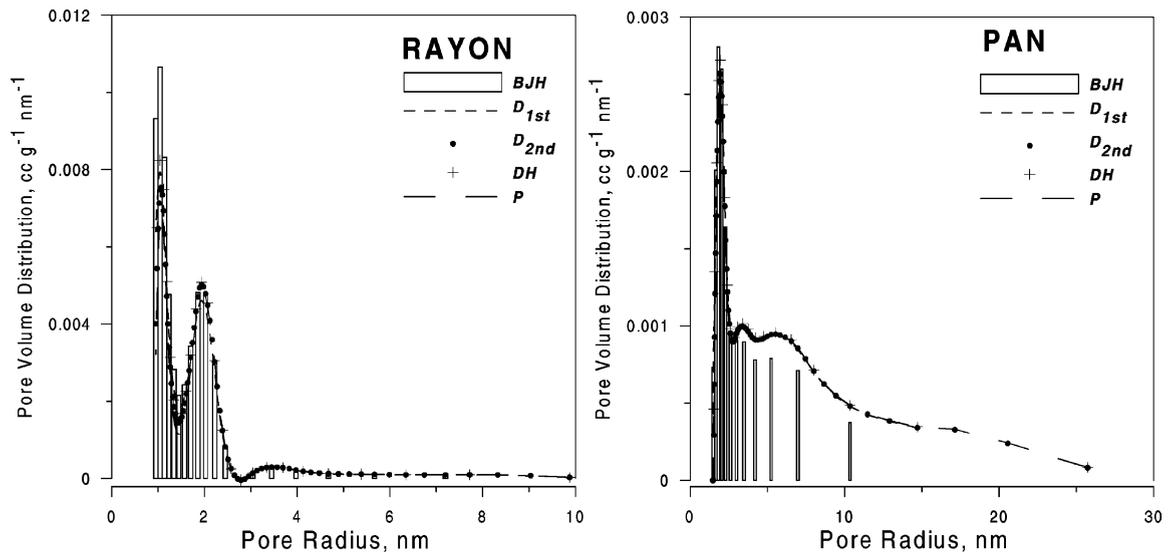
Fig. 2. MPSDs of Rayon and PAN activated carbon fibers obtained by means of classical iterative methods (i.e. Barrett, Joyner and Halenda (*BJH*), Dubinin (the so-called first variant—D_{1ST} and the so-called second variant—D_{2ND}), Dollimore and Heal (*DH*), and Pierce (*P*)).

Finally, both the samples were also characterized by using a fractal geometry approach. The fractal dimension of the surface ($2 \leq D < 3$) accessible for adsorption is an operative measure of the surface irregularity [39–53]. Calculating of the fractal dimension of the ACFs was performed on the basis of adsorption data in the capillary condensation region using the fractal analog of Frenkel–Halsey–Hill equation (*FHH* method) [44,45,48,49]:

$$\frac{a}{a_{\mathrm{m}}} = \kappa[\ln(p_{\mathrm{s}}/p)]^{-1/m}, \quad \text{and} \quad m = 1/(3 - D) \quad (23)$$

where a is the amount adsorbed at a given relative pressure p/p_{s}, a_{m} the amount required to form a adsorbed monolayer coverage (taken usually from Brunauer–Emmett–Teller (*BET*) equation) [54,55], and κ is a constant.

4. Results and discussion

The experimental nitrogen adsorption–desorption isotherms at 77.5 K on PAN and Rayon activated
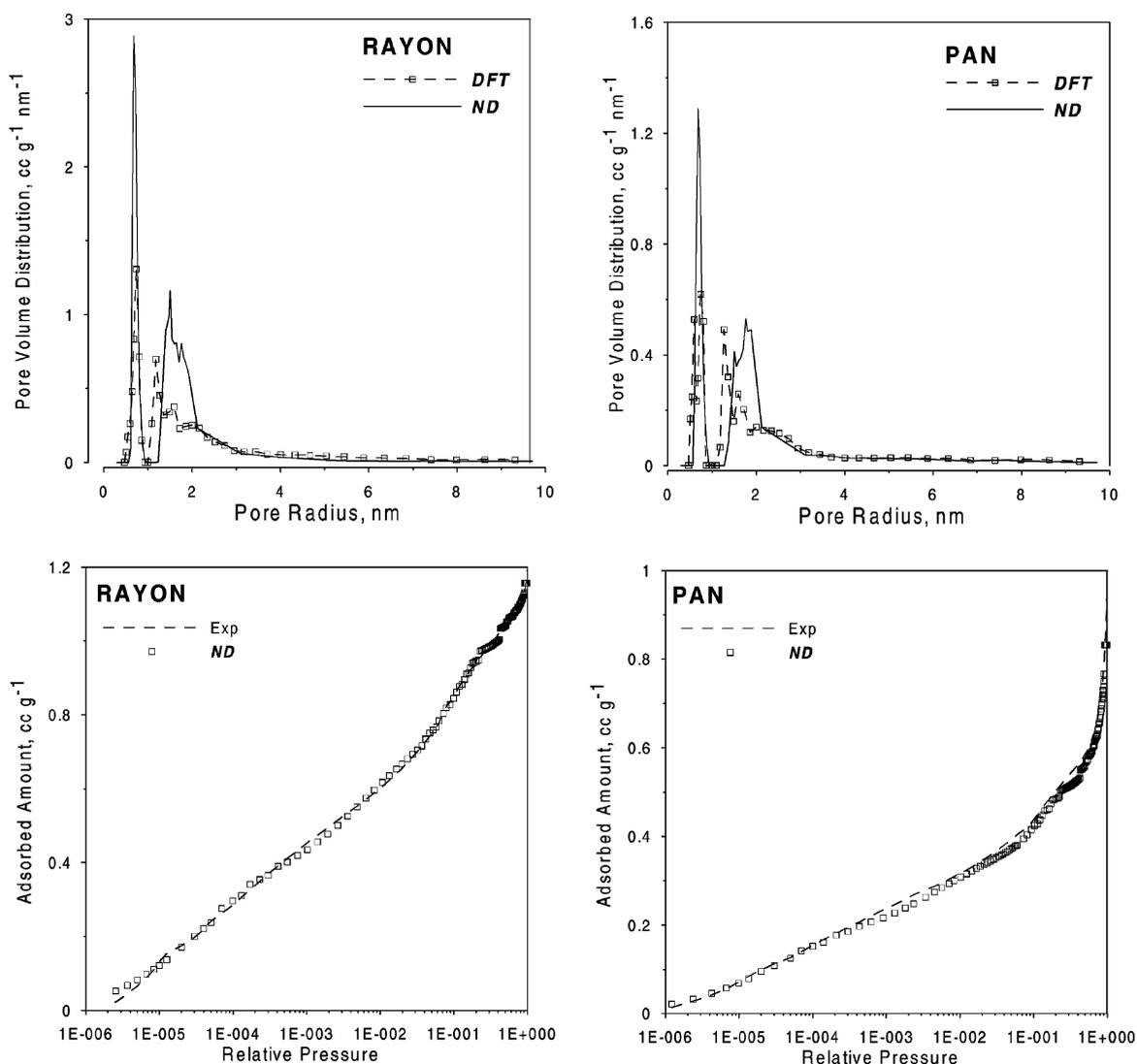

Fig. 3. The comparison of *DFT* and *ND* pore size distributions for the samples studied, and the fit of *ND* method to experimental data (Exp).

carbon fibers are shown in Fig. 1. Both isotherms are characterized by the presence of hysteresis loop in the condensation capillary region (i.e. these samples of ACFs possess considerable contribution of mesopores). Additionally, from Fig. 1 it is clearly seen that these samples of ACFs differ significantly, in terms of total pore volume as well as pore structure. The basic parameters describing of ACFs properties were obtained by applying the methods described in the previous section and *n-BET* and *FHH* equations (see Table 1). It can be noticed that the mesopore surface area of Rayon activated carbon fiber is two times greater than that of PAN ACF, while the mesopore volumes are comparable. All iterative methods developed on the ground of both Kelvin and *t*-curve equations give similar result of mesopore size distributions (Fig. 2). Rayon is characterized by a bi-porous structure of MPSDs. The main fraction of mesopores is located in the range 1–1.5 nm of pore radius. The second peak appears around a pore radius of 2 nm. PAN is characterized by considerably greater quantity of larger mesopores (i.e. greater than 5 nm).

Fig. 3 shows that the most advanced method of porosity characterization, proposed by Nguyen and Do, gives similar results as those obtained from *DFT* analysis. This was also observed for other systems mainly for microporous and mesoporous ones [25–32,56].

The main difference is the intensity of the peak located at 2 nm. In both the cases *ND* method leads to a larger intensity of this peak, and a small shift towards larger pore diameters. As it can be seen in Fig. 3, the fit of the *ND* method to experimental isotherms is very good, and this leads to the conclusion that, proposed in this paper, the numerical procedure (ASA) of fitting the model to experimental data is very effective.

In Fig. 4, MPSDs obtained by the method proposed by Do are shown. It can be noticed that this method leads to a more regular MPSD curve. Both PAN and Rayon are characterized by a single peak but the dimension and quantity of mesopores differ significantly. As it was concluded from the results of the methods presented above this method also shows that PAN is characterized by a larger quantity of wider mesopores (i.e. pore radius >4 nm). The results obtained from adsorption and desorption data are very similar for both solids in this case.

Interesting results are shown in Fig. 5 where the comparison of the results obtained from the *ND* and *DBdBDDU* methods is presented. Although it may seem strange, MPSDs obtained from the *ND* (and *DFT*) and *DBdbDDU* methods are almost the same. In the current study, only two adsorbents were analysed. Thus, it is hard to postulate that the both methods always lead to the same results, however,
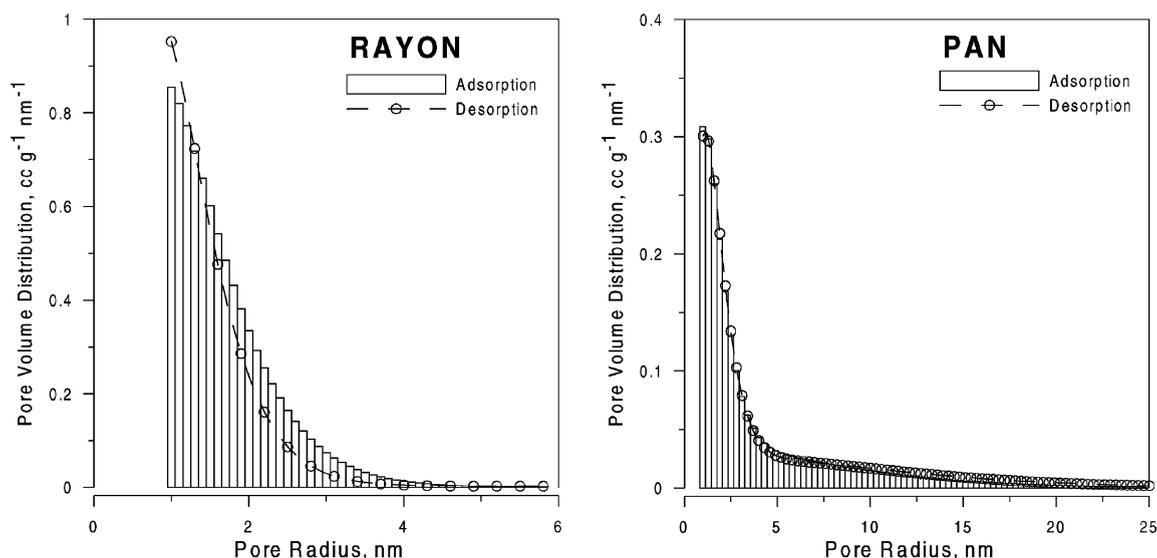

Fig. 4. MPSDs of Rayon and PAN activated carbon fibers obtained from both adsorption (Adsorption) and desorption (Desorption) branch of nitrogen adsorption–desorption isotherms at 77.5 K by means of method described by Do (*Do* method).
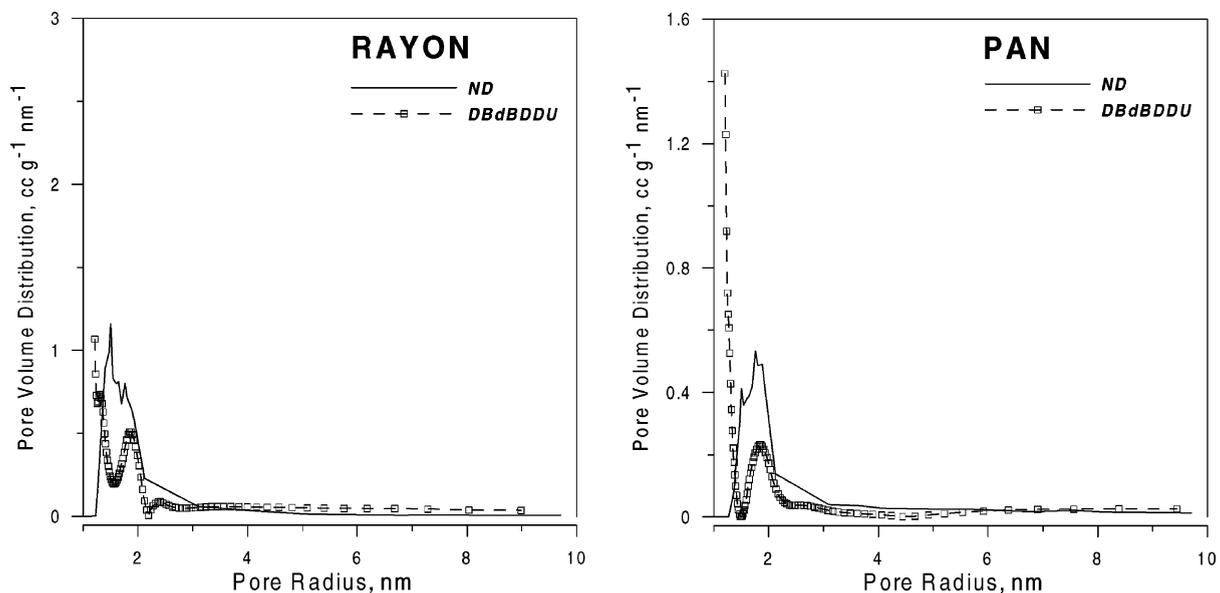
Fig. 5. MPSDs of Rayon and PAN activated carbon fibers obtained by means of methods: *DBdBDDU*—Derjaguin–Broekhoff–deBoer–Dollimore–Dubinin–Ulin, *ND*—Nguyen and Do.

it seems to be very probable. Thus, in the case of the studied systems, and for the range of mesopores, the time-consuming and advanced mathematically *DFT* and or *ND* methods can be effectively replaced with a simpler *DBdBDDU* method.

Fig. 6 shows that the fit of *BET* and *FHH* fractal analog to the experimental data is good. However, for Rayon carbon, which is more heterogeneous, the fit for *FHH* equation is worse. The value of the surface fractal dimension for the two samples of
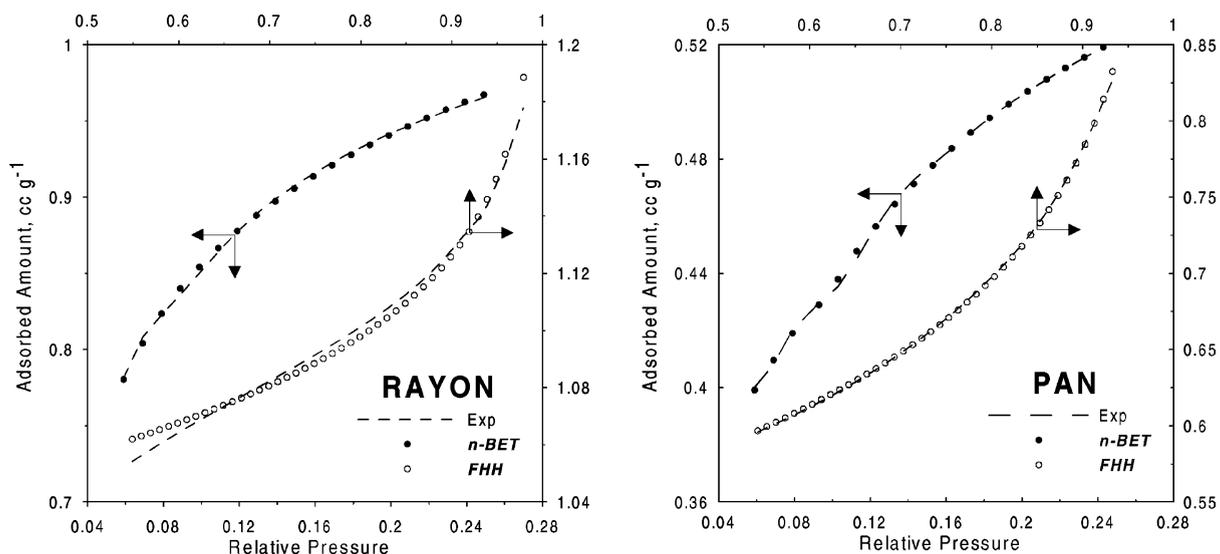

Fig. 6. Adsorption of nitrogen in mesopores of PAN and Rayon activated carbon fibers: Exp—experimental points, fitting by Brunauer–Emmett–Teller (*n-BET*) equation, and fitting by fractal Frenkel–Halsey–Hill (*FHH*) equation.

ACFs is high. This suggests large surface heterogeneity.

5. Conclusions

The mesopore volumes calculated from different models are comparable, while larger differences are observed in the values of pore surface area. All iterative methods lead to similar mesopore size distribution curves. Do's method leads to a more regular PSD curve as obtained from iterative methods, and the differences between the results calculated from adsorption and desorption branches of isotherm are small. The most sophisticated methods of porosity characterization, namely *DFT* and *ND* lead to practically the same results, and small differences are observed in the intensity of the peak located in the upper range of micropores. The new numerical strategy of fitting of *ND* method to experimental data is very effective and can be successfully used for the characterization of porous carbonaceous materials.

The method proposed by Derjaguin–Broekhoff and de Boer, modified by Dubinin and Ulin is probably the most sophisticated method among older methods of mesoporosity characterization. It leads to almost the same results as *DFT* and *ND*. Thus, in the range of mesoporosity characterization, for carbons the time-consuming and advanced methods can be effectively replaced with a very simple one. Since only two mesoporous adsorbents are studied in the current paper the question arises about the comparable results of these two methods for other systems. This will be the subject of our future correspondence.

References

[1] L.H. Peebles, Carbon Fibers: Formation, Structure, and Properties, CRC Press, Boca Raton, 1995.
[2] N. Murdie, Carbon fiber/carbon composites: production, properties and applications, in: H. Marsh, E.A., Heintz, F. Rodriguez-Reinoso (Eds.), Introduction to Carbon Technologies, Universidad, Alicante, 1997.
[3] K. Kaneko, C. Ishii, H. Kanoh, Y. Hanzawa, N. Setoyama, T. Suzuki, Adv. Colloid Interf. Sci. 76–77 (1998) 295.
[4] Z. Ryu, J. Zheng, M. Wang, Carbon 36 (1998) 427.
[5] Z. Ryu, J. Zheng, M. Wang, B. Zhang, Carbon 37 (1999) 1257.
[6] M. Suzuki, Carbon 32 (1994) 577.
[7] K. Kaneko, J. Membr. Sci. 96 (1996) 59.
[8] H. Tamai, T. Kakii, Y. Hirota, T. Kumamoto, H. Yasuda, Chem. Mater. 8 (1996) 456.
[9] E.P. Barrett, L.G. Joyner, P.H. Halenda, J. Am. Chem. Soc. 73 (1951) 373.
[10] M.M. Dubinin, J.G. Zhukovskaya, Zhur. Fiz. Khim. 30 (1956) 1840.
[11] M.M. Dubinin, L.I. Kataeva, Izv. Akad. Nauk SSSR., Ser. Khim. 3 (1980) 498.
[12] D. Dollimore, G.R. Heal, J. Colloid Interf. Sci. 33 (1970) 508.
[13] C. Pierce, J. Phys. Chem. 57 (1953) 149.
[14] J. Jagiełło, J. Klinik, Chemia Stosowana 24 (1980) 331 (in Polish).
[15] J. Klinik, The Comparison of various methods used for the determination of mesopore structure of porous solids, in: J. Rouquerol, F. Rodriguez-Reinoso, K.S.W. Sing, K.K. Unger (Eds.), Characterization of Porous Solids III, Studies in Surface Science and Catalysis, vol. 87, 1994.
[16] B.V. Derjaguin, J. Colloid Interf. Sci. 24 (1967) 357.
[17] J.C.P. Broekhoff, J.H. de Boer, J. Catal. 9 (1967) 8.
[18] J.C.P. Broekhoff, J.H. de Boer, J. Catal. 9 (1967) 15.
[19] J.C.P. Broekhoff, J.H. de Boer, J. Catal. 10 (1968) 153.
[20] J.C.P. Broekhoff, J.H. de Boer, J. Catal. 10 (1968) 368.
[21] J.C.P. Broekhoff, J.H. de Boer, J. Catal. 10 (1968) 377.
[22] J.C.P. Broekhoff, J.H. de Boer, J. Catal. 10 (1968) 391.
[23] A.J. Lecloux, Catalysis—Science and Technology, vol 2, Akademie Verlag, Berlin, 1983.
[24] M.M. Dubinin, L.I. Kataeva, V.I. Ulin, Izv. Akad. Nauk SSSR., Ser. Khim. 3 (1977) 510.
[25] C. Nguyen, D.D. Do, Langmuir 15 (1999) 3608.
[26] C. Nguyen, D.D. Do, Langmuir 16 (2000) 1319.
[27] C. Nguyen, D.D. Do, Carbon 39 (2001) 1327.
[28] D.D. Do, C. Nguyen, H.D. Do, Colloids Surf. A. 187–188 (2001) 51.
[29] V.M. Gun'ko, D.D. Do, Colloids Surf. A. 193 (2001) 71.
[30] D.D. Do, H.D. Do, Appl. Surf. Sci. 7821 (2002) 1.
[31] D.D. Do, H.D. Do, Langmuir 18 (2002) 93.
[32] P. Kowalczyk, A.P. Terzyk, P.A. Gauden, R. Leboda, E. Szmechtig-Gauden, G. Rychlicki, Z. Ryu, H. Rong, Carbon, submitted for publication.
[33] P.I. Ravikovitch, A. Vishnyakov, R. Russo, A.V. Neimark, Langmuir 16 (2000) 2311.
[34] Z. Michalewicz, D. Fogel, How to Solve It: Modern Heuristics, Springer Verlag, Berlin, 2000.
[35] P. Kowalczyk, L. Solarz, A.P. Terzyk, P.A. Gauden, R. Leboda, V.M. Gun'ko, Shedae Infoematicae, submitted for publication.
[36] H.P. Schwefel, Evolution and Optimum Seeking, Wiley, Chichester, 1995.
[37] Z. Michalewicz, Genetic Algorithms + Data Structures = Evolution Programs, Springer Verlag, Berlin, 1996.
[38] D.D. Do, Adsorption Analysis: Equilibria and Kinetics, Imperial College Press, London, 1998.
[39] P. Pfeifer, D. Avnir, J. Chem. Phys. 79 (1983) 3553.
[40] K. Kaneko, M. Sato, T. Suzuki, Y. Fujiwara, K. Nishikawa, M. Jaroniec, J. Chem. Soc., Faraday Trans. 87 (1991) 1991.

[41] R. Leboda, M. Marciniak, V.M. Gun'ko, W. Grzegorczyk, A.A. Malygin, A.A. Malkov, Colloids Surf. A 167 (2000) 275.
[42] R. Leboda, V.M. Gun'ko, M. Marciniak, A.A. Malygin, A.A. Malkin, W. Grzegorczyk, B.J. Trznadel, E.M. Pakhlov, E.F. Voronin, J. Colloid Interf. Sci. 218 (1999) 23.
[43] M. Jaroniec, M. Kruk, J. Olivier, Surf. Sci. 342 (1995) L1130.
[44] Y. Yin, Langmuir 7 (1991) 216.
[45] M.W. Cole, N.S. Holter, P. Pfeifer, Phys. Rev. 33 (1986) 8806.
[46] R. Tsunoda, J. Colloid Interf. Sci. 182 (1996) 306.
[47] Z. Sokołowska, A. Patrykiejew, S. Sokołowski, Pol. J. Chem. 64 (1990) 711.
[48] W. Rudziński, S.-L. Lee, C.-C.S. Yan, T. Panczyk, J. Phys. Chem. B 105 (2001) 10847.
[49] W. Rudziński, S.-L. Lee, T. Panczyk, C.-C.S. Yan, J. Phys. Chem. B 105 (2001) 10857.
[50] A.P. Terzyk, P.A. Gauden, G. Rychlicki, R. Wojsz, Langmuir 15 (1999) 285.
[51] A.P. Terzyk, P.A. Gauden, G. Rychlicki, R. Wojsz, Colloids Surf. A 152 (1999) 293.
[52] A.P. Terzyk, P.A. Gauden, G. Rychlicki, Carbon 39 (2001) 267.
[53] P.A. Gauden, A.P. Terzyk, G. Rychlicki, P. Kowalczyk, J. Colloid Interf. Sci. 244 (2001) 439.
[54] F. Meng, J.R. Schlup, L.T. Fan, J. Colloid Interf. Sci. 88 (1998) 88.
[55] S. Lowell, J.E., Powder Surface Area and Porosity, Chapters 1, 4, 9 Chapman & Hall, New York, 1984.
[56] P. Kowalczyk, A.P. Terzyk, P.A. Gauden, V.M. Gun'ko, J. Colloid Interf. Sci., in press.